Accepted Manuscript

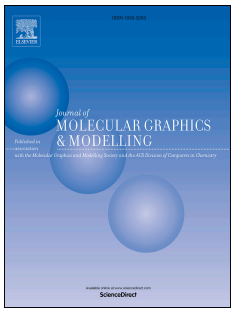

An experimental and DFT study of the packing and structure of dithenoylmethane monocarbonylphosphine Rhodium(I) complex [Rh((C_4H_3S)COCHCO(C_4H_3S)) (CO) (PPh_3)]

Marrigje Marianne Conradie, Petrus H.van Rooyen

PII: S1093-3263(18)30131-1

DOI: 10.1016/j.jmgm.2018.04.016

Reference: JMG 7161

To appear in: *Journal of Molecular Graphics and Modelling*

Received Date: 23 February 2018

Revised Date: 24 April 2018

Accepted Date: 25 April 2018

Please cite this article as: M.M. Conradie, P.H.v. Rooyen, An experimental and DFT study of the packing and structure of dithenoylmethane monocarbonylphosphine Rhodium(I) complex [Rh((C_4H_3S)COCHCO(C_4H_3S)) (CO) (PPh_3)], *Journal of Molecular Graphics and Modelling* (2018), doi: 10.1016/j.jmgm.2018.04.016.

An experimental and DFT study of the Packing and Structure of Dithenoylmethane Monocarbonylphosphine Rhodium(I) complex [Rh((C_4H_3S)COCHCO(C_4H_3S))(CO)(PPh_3)].

Marrigje Marianne Conradie,*[a] Petrus H.van Rooyen[b]

[a] Department of Chemistry, PO Box 339, University of the Free State, 9300 Bloemfontein, Republic of South Africa.

[b] Department of Chemistry, University of Pretoria, Private Bag X20, Hatfield, 0028, South Africa.

*Contact author details:

Name: Marrigje Marianne Conradie

Tel: +27-51-4019898

Fax: +27-51-4017295

E-mail: ConradieMM@ufs.ac.za

Keywords

Rhodium; DFT; thienyl unit; QTAIM; NBO; intermolecular interactions

Graphical abstract

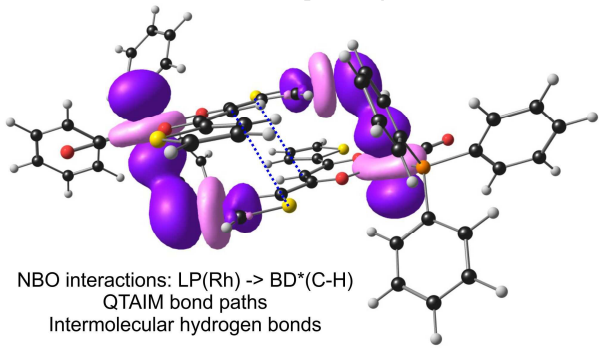

DFT calculations give electronic understanding of experimental crystal packing of [Rh((C$_4$H$_3$S)COCHCO(C$_4$H$_3$S))(CO)(PPh$_3$)].

Highlights

Packing in pairs with weak intermolecular interaction

AIM bonding paths indicating intermolecular bonding paths

NBO shows intermolecular donor-acceptor interaction

Abstract

[Rh((C$_4$H$_3$S)COCHCO(C$_4$H$_3$S))(CO)(PPh$_3$)] crystals stack in one dimensional linear chains in the solid state, with slightly slipped π-stacking of the thienyl groups of one molecule and the β-diketonato backbone of a neighbouring molecule. The observed stacking is possible due to the near planar orientation of the two aromatic thienyl groups and the β-diketonato backbone. The experimentally observed stacking and close intermolecular contacts are in agreement with theoretical QTAIM calculated intermolecular bond paths and intermolecular hydrogen bonds between neighbouring molecules. NBO calculations revealed donor – acceptor NBO interactions between the lone pair on rhodium of one molecule and (i) the empty antibonding orbital on C-H of the nearest thienyl group of a neighbouring molecule, as well as with the (ii) the empty antibonding orbital on two carbons of the nearest thienyl group to rhodium on the neighbouring molecule.

1 Introduction

Thiophene is a heterocyclic compound, consisting of a planar five-membered ring with the formula C$_4$H$_4$S. When deprotonated, thiophene is converted into the thienyl group (C$_4$H$_3$S)$^-$, which is widely used as a building block in various chemicals. Thiophene containing chemicals has a wide application in agrochemicals and pharmaceuticals, even though these chemicals rarely occur in plants and do not have a role in animal metabolism [1]. When thiophenes are linked in the 2- and 5-positions, they form sulphur containing heterocyclic species called oligiothiophenes. When electrons are added or removed from the conjugated π-orbitals, these oligiothiophenes become conductive. The oligiothiophene-metal complexes are appealing to be investigated with regards to

the conductivity of materials, with the application as active layers in molecular electronics. The bidentate group, β-diketone, is a practical end-capping unit to anchor transition metals, with the thiophene as a terminus on the β-diketone ligand. Synthesizing these oligiothiophene-metal complexes serves as an important class of new materials of which the properties can be adapted to fine tune the coupling of the electronic properties of the metal versus the π-conjugated system [2].

In this contribution we report the crystal structure of a thienyl containing rhodium(I) complex, [Rh((C$_4$H$_3$S)COCHCO(C$_4$H$_3$S))(CO)(PPh$_3$)]. This complex stacks in one dimensional linear chains in the solid state, with slightly slipped π-stacking of the thienyl groups of one molecule and the β-diketonato backbone of a neighbouring molecule, see Scheme 1 for the structure. The experimentally observed intermolecular interaction between the thienyl groups, is further studied by a density functional study to understand the interaction between two molecules, as noted in the observed experimental packing of the molecules.

2 Experimental

2.1 Synthesis

[Rh((C$_4$H$_3$S)COCHCO(C$_4$H$_3$S))(CO)(PPh$_3$)] was synthesized from 1,3-di(2-thenoyl)-1,3-propanedione [3] and RhCl$_3$.xH$_2$O as described in literature [4,5]. Characterization data for [Rh((C$_4$H$_3$S)COCHCO(C$_4$H$_3$S))(CO)(PPh$_3$)]:

Yield: 0.0662 g, 52.7%. M.p. 180.0-184.5 °C. IR (cm^{-1}) = 1971. ^{1}H NMR (δ/ppm, CDCl$_3$) 6.65 (1H, s, CH), 6.89 (1H, dd, ^3J = 5 Hz, ^3J = 4 Hz, ring B CH), 7.08 (1H, dd, ^3J = 4 Hz, ^4J = 1 Hz, ring B CH), 7.11 (1H, dd, ^3J = 5 Hz, ^3J = 4 Hz, ring A CH), 7.27 (1H, dd, ^3J = 5 Hz, ^4J = 1 Hz, ring B CH), 7.41 (6H, m, CH), 7.45 (3H, m, CH), 7.52 (1H, dd, ^3J = 5 Hz, ^4J = 1 Hz, ring A CH), 7.73 (1H, dd, ^3J = 4 Hz, ^4J = 1 Hz, ring A CH), 7.74 (6H, m, CH). Elemental *Anal*. Calc. for RhC$_{30}$PH$_{22}$S$_2$O$_3$: C, 57.3; H, 3.5. Found: C, 57.0; H, 3.2%.

2.2 Crystal structure analysis

Data for [Rh((C$_4$H$_3$S)COCHCO(C$_4$H$_3$S))(CO)(PPh$_3$)] was collected at 150K on a Bruker D8 Venture kappa geometry diffractometer, with duo Iμs sources, a Photon 100 CMOS detector and APEX II [6] control software, using Quazar multi-layer optics, monochromated Mo-*K*α radiation, by means of a combination of ϕ and ω scans. Data reduction was performed using SAINT+ [6] and

the intensities were corrected for absorption, using SADABS [6]. The structure was solved by intrinsic phasing, using SHELXTS, and refined by full-matrix least squares, using both SHELXTL+ [7] and SHELXL-2017+ [7]. In the structure refinement, all hydrogen atoms were added in the calculated positions and treated as riding on the atom to which they are attached. All non-hydrogen atoms were refined with anisotropic displacement parameters; all isotropic displacement parameters for hydrogen atoms were calculated as ($X \times U_{eq}$) of the atom to which they are attached, where X = 1.2 for all hydrogen atoms. Crystal data, data collection, structure solution and refinement details are available in the CIF (CCDC deposit number 1811145).

2.3 Theoretical approach

Density functional theory (DFT) calculations of this study done with the Gaussian 09 program package [8]. A selection of functionals were used, namely the GGA (Generalized Gradient Approximation) functional PW91 [9] and LC-BLYP [10,11,12,13] (long range corrected BLYP), meta-GGA functional M06-D3 [14] (M06 with the Grimme empirical dispersion correction D3 [15]) and the hybrid functionals B3LYP (Becke 1993 and Lee-Yang-Parr) [16,17] and CAM-B3LYP [18] (long range corrected version of B3LYP), with the triple-ζ basis set 6-311G(d,p) basis for the lighter atoms (C, H, N, O, S, P), and the LANL2DZ basis set (corresponding to the Los Alamos Effective Core Potential plus DZ) [19] for Rh. The 6-311G(d,p)/LANL2DZ basis set proved to give reliable geometries and energies for rhodium-β-diketonato complexes [20,21,22]. The LC-BLYP optimised gas phase structures were used to further conduct a natural bond orbital (NBO) analysis (using the NBO 3.1 module [23] in Gaussian 09), as well as an electronic density analysis (using Bader's quantum theory of atoms in molecules (QTAIM) [24,25,26], as implemented in ADF2017 [27,28,29]). The single molecular unit [Rh((C$_4$H$_3$S)COCHCO(C$_4$H$_3$S))(CO)(PPh$_3$)], as well as two [Rh((C$_4$H$_3$S)COCHCO(C$_4$H$_3$S))(CO)(PPh$_3$)] units near to each other, were optimized. The input coordinates for the latter were obtained from the crystal data, also presented in this study. The optimized coordinates of the DFT calculations are provided in the Supporting Information.

2.4 Software

Mercury [30,31] was used to produce **Figure 1**, **Figure 2**, **Figure 6** and **Figure 7**. Chemcraft [32] was used to produce **Figure 4**. ADF GUI [29] were used to produce **Figure 5**.

3.1 Synthesis

The synthesis route for [Rh((C$_4$H$_3$S)COCHCO(C$_4$H$_3$S))(CO)(PPh$_3$)] is shown Scheme 1. A DMF solution of RhCl$_3$.xH$_2$O was heated with the formation of [NH$_2$(CH$_3$)$_2$]$^+$[Rh(CO)$_2$Cl$_2$]$^-$ [33]. 1,3-di(2-thenoyl)-1,3-propanedione [3] was added *in situ* to the reaction mixture with the formation of [Rh((C$_4$H$_3$S)COCHCO(C$_4$H$_3$S))(CO)$_2$]. [Rh((C$_4$H$_3$S)COCHCO(C$_4$H$_3$S))(CO)$_2$] was isolated, air dried and recrystallized from chloroform. [Rh((C$_4$H$_3$S)COCHCO(C$_4$H$_3$S))(CO)$_2$] was dissolved in chloroform, a solution of PPh$_3$ in chloroform was added, the reaction mixture stirred for until no more CO gas was released with the precipitation of [Rh((C$_4$H$_3$S)COCHCO(C$_4$H$_3$S))(CO)(PPh$_3$)]. [Rh((C$_4$H$_3$S)COCHCO(C$_4$H$_3$S))(CO)(PPh$_3$)] was isolated, air dried and recrystallized from *n*-hexane.

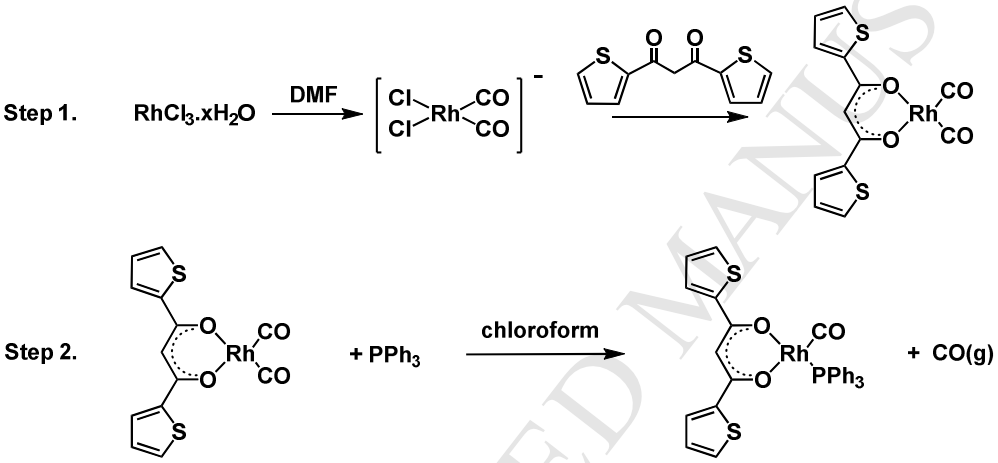

Scheme 1. Synthesis of [Rh((C$_4$H$_3$S)COCHCO(C$_4$H$_3$S))(CO)(PPh$_3$)].

3.2 X-ray structure

A molecular diagram of [Rh((C$_4$H$_3$S)COCHCO(C$_4$H$_3$S))(CO)(PPh$_3$)] is presented in **Figure 1**, while crystal data and structure refinement are summarised in **Table 1**. **Table 2** compares selected geometrical data of the crystals from this study with related [Rh(R^{1}COCHCOR^2)(CO)(PPh$_3$)] complexes, (R^{1}COCHCOR^2)$^-$ = β-diketonato ligand with side groups R^1 and R^2 [34]. Additional crystallographic data are provided in the supplementary information.

Due to a rotational disorder, the thienyl rings occur in two orientations in the structure. The major orientation observed is with both S-atoms in a *cis*-orientation relative to the closest O-atoms, that is S1 *cis* to O1 and S2 *cis* to O2. The refined ratios for the site occupancies are 0.802 for S1:C3A and

0.931 for S2:C9A. The data for major conformer was used in the structural analysis. The orientation of the two aromatic thienyl groups on the β-diketonato backbone of [Rh((C$_4$H$_3$S)COCHCO(C$_4$H$_3$S))(CO)(PPh$_3$)] deviates very slightly from the plane through the β-diketonato backbone. The planes containing the thienyl groups deviate by 4.7(2)° and 3.5(2)° from plane that includes only the β-diketonato moiety. The bond lengths and angles of the bonds and angles round rhodium, as well as the C-C bonds of the β-diketonato backbone of [Rh((C$_4$H$_3$S)COCHCO(C$_4$H$_3$S))(CO)(PPh$_3$)] are very similar to the average lengths in related [Rh(R^{1}COCHCOR^2))(CO)(PPh$_3$)] structures (**Table 2**). The C1-C6 and C6-C7 bonds, the C1-O1 and C7-O2 bonds, as well as the Rh-O1 and Rh-O2 bonds, in each [Rh(R^{1}COCHCOR^2))(CO)(PPh$_3$)] molecule, are generally very similar, leading to conjugation through the pseudo aromatic β-diketonato backbone. This conjugation allows for good electronic communication between the R^1 and R^2 groups and rhodium.

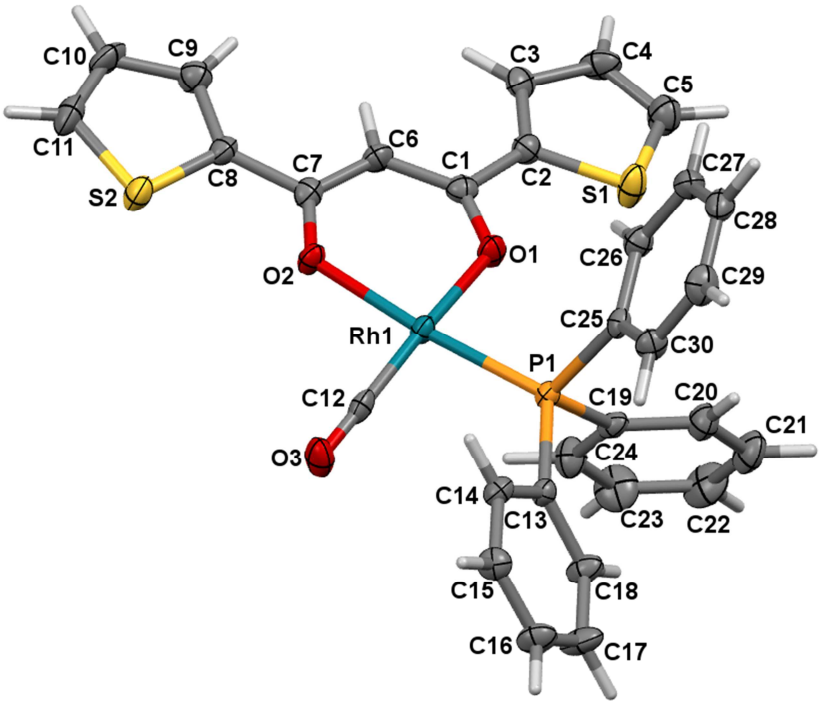

Figure 1: A perspective drawing of the molecular structure of [Rh((C$_4$H$_3$S)COCHCO(C$_4$H$_3$S))(CO)(PPh$_3$)] showing the atom numbering scheme. Both thienyl groups displayed orientational disorder in the position of the sulfur-atoms of thienyl-ring (80 and 90%), the major conformation is shown. Atomic displacement parameters (ADPs) are shown at the 50 % probability level.

Table 1: Crystal data and structure refinement of [Rh((C$_4$H$_3$S)COCHCO(C$_4$H$_3$S))(CO)(PPh$_3$)].

Empirical formula	C30 H22 O3 P Rh S2
Formula weight	628.47
Temperature	150(2) K
Wavelength	0.71073 Å
Crystal system	Triclinic
Space group	P -1
Unit cell dimensions	a = 8.9164(5) Å b = 10.0741(6) Å c = 14.9025(9) Å a= 83.584(3)°. b= 83.702(3)°. g = 86.035(3)°.
Volume	1320.01(13) Å^3
Z	2
Density (calculated)	1.581 Mg/m^3
Absorption coefficient	0.897 mm^{-1}
F(000)	636
Crystal size	0.240 x 0.160 x 0.100 mm^3
Theta range for data collection	2.302 to 25.345°.
Index ranges	-10<=h<=10, -12<=k<=12, -17<=l<=17
Reflections collected	23014
Independent reflections	4832 [R(int) = 0.0540]
Completeness to theta = 25.242°	99.9 %
Refinement method	Full-matrix least-squares on F^2
Data / restraints / parameters	4832 / 0 / 348
Goodness-of-fit on F^2	1.089
Final R indices [I>2sigma(I)]	R1 = 0.0327, wR2 = 0.0777
R indices (all data)	R1 = 0.0396, wR2 = 0.0808
Extinction coefficient	n/a
Largest diff. peak and hole	0.827 and -0.331 e.Å^{-3}

Table 2: Selected geometrical data (bond lengths in Å and bond angles in degrees) of [Rh(R^1COCHCOR^2)**)**(CO)(PPh_3)] complexes. Atom numbering according to **Figure 1**.

R^1 (*trans* PPh_3)	R^2 (*trans* CO)	Rh-P	Rh-C_{CO}	Rh-$O2_{trans\ PPh3}$	Rh-$O1_{cis\ PPh3}$	C1-O1	C1-C6	C6-C7	C7-O2	P-Rh-C_{CO}	O1-Rh-O2	CSD Refcode
CH_3	CH_3	2.243	1.801	2.086	2.029	1.273	1.397	1.381	1.274	87.79	87.92	ACRHCP
CH_3	CH_3	2.242	1.807	2.075	2.033	1.275	1.396	1.394	1.273	87.18	88.02	ACRHCP01
CF_3	$CH(CH_3)_2$	2.239	1.781	2.057	2.088	1.285	1.361	1.408	1.271	87.25	87.54	CAPSER
CF_3	^{t}Bu	2.237	1.765	2.062	2.071	1.257	1.383	1.412	1.267	91.25	88.12	DUWHIM
CF_3	Et	2.252	1.796	2.047	2.094	1.257	1.380	1.413	1.291	88.12	87.57	FODJEN
Ph	$(CH_2)_2$Et	2.254	1.791	2.033	2.076	1.275	1.396	1.394	1.283	92.05	88.87	KEXCEX
CF_3	Fc	2.232	1.801	2.070	2.048	1.266	1.412	1.368	1.264	92.71	88.63	KUNBIE
Et	Ph	2.238	1.796	2.061	2.032	1.289	1.382	1.390	1.263	88.15	89.39	OJEWOQ
Ph	Et	2.239	1.788	2.032	2.068	1.285	1.375	1.380	1.282	87.45	87.84	OJEWOQ
Ph	Ph	2.236	1.813	2.081	2.037	1.263	1.388	1.378	1.274	91.13	88.51	ROGVEO
Ph	Ph	2.245	1.794	2.072	2.039	1.298	1.374	1.419	1.274	91.82	89.10	ROGVEO
Th	CF_3	2.245	1.781	2.052	2.085	1.261	1.432	1.345	1.288	87.08	87.56	TFAPRH
Ph	CH_2Et	2.241	1.794	2.064	2.062	1.277	1.399	1.393	1.280	92.45	87.96	YIHWUJ
CH_3	Ph	2.249	1.739	2.078	2.032	1.270	1.427	1.281	1.287	88.92	88.13	ZAWQAP
Ph	CH_3	2.248	1.768	2.019	2.057	1.339	1.397	1.274	1.249	86.95	86.13	ZAWQAP
Th	Th	2.2393(7)	1.802(3)	2.0798(18)	2.0355(19)	1.289(3)	1.386(4)	1.399(4)	1.278(3)	91.24(9)	89.11(7)	this study
	ave	2.242	1.789	2.061	2.055	1.279	1.393	1.377	1.275	89.471	88.149	
	max	2.254	1.813	2.086	2.094	1.339	1.432	1.419	1.291	92.712	89.388	
	min	2.232	1.739	2.019	2.029	1.257	1.361	1.274	1.249	86.951	86.126	

The near planar orientation of the two aromatic thienyl groups and the β-diketonato backbone leads to stacking of [Rh((C$_4$H$_3$S)COCHCO(C$_4$H$_3$S))(CO)(PPh$_3$)] in one dimensional linear chains in the solid state, with slightly slipped π-stacking of the thienyl groups and the β-diketonato backbone (**Figure 2**. (a)). The centroid(β-diketonato)-centroid(thienyl) distances are 3.753(2) Å for the thienyl ring including S1, and 4.797(2) Å for the thienyl ring that includes S2. Each β-diketonato moiety is involved in two different π-π interactions, the most dominating one clearly being with the thienyl ring that includes S1 where the inter-centroid distance is shorter at 3.753(2) Å. However, the secondary but weaker π-π interaction, with the thienyl ring that includes S2, also contributes to directing the packing as mainly a one-dimensional chain. The orientation of the phenyl rings leads to intermolecular hydrogen bonding interactions, see **Figure 2** (b).

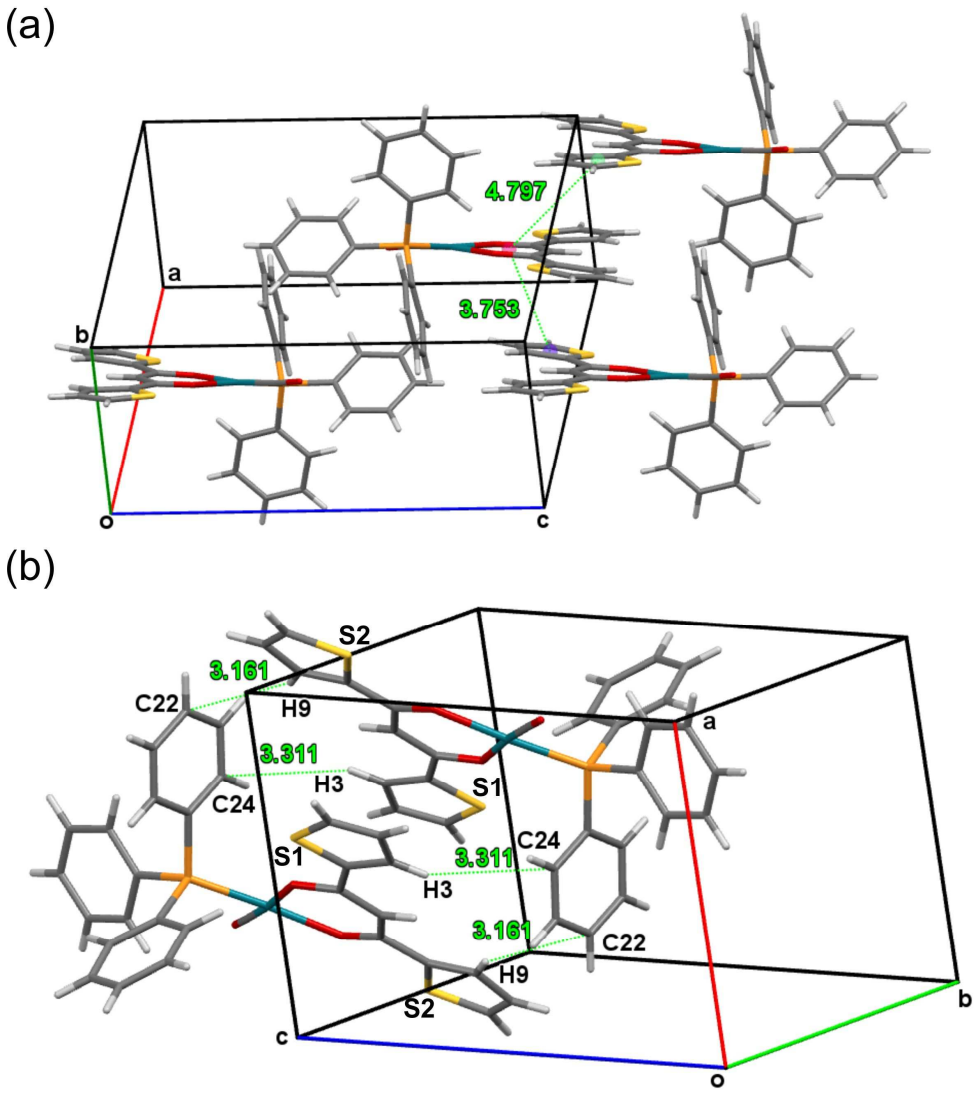

Figure 2: Packing of [Rh((C$_4$H$_3$S)COCHCO(C$_4$H$_3$S))(CO)(PPh$_3$)] with (a) selected π-π interactions and (b) intermolecular interactions shown.

3.3 Computational chemistry

3.3.1 Single [Rh((C$_4$H$_3$S)COCHCO(C$_4$H$_3$S))(CO)(PPh$_3$)] molecule.

The single [Rh((C$_4$H$_3$S)COCHCO(C$_4$H$_3$S))(CO)(PPh$_3$)] molecule was optimized with a selection of functionals (B3LYP, PW91, M06-D3, LC-BLYP and CAM-B3LYP). GGA, meta-GGA and hybrid functionals were used, some long range or dispersion corrected, in order to find the best functional to reproduce the experimentally observed structures. The bond lengths and bond angles around the rhodium centre, a key indicator of the structure in organometallic complexes, are summarized in **Table 3**. Compared to the experimental crystal, all of the selected functionals managed to produce a good geometry of the single molecule. The calculated bond lengths around the rhodium centre deviated with maximum 0.07 Å from the experimental crystal and the bond angles deviated with maximum 3.5°. The slight overestimation of DFT calculated metal-ligand bond lengths was expected, as this is generally observed for gas phase calculations [35], and thus considered as insignificant. This is also in agreement with previously studied related rhodium-β-diketonato complexes, where the gas phase optimisations relative to the experimental crystal data resulted in slightly overestimated rhodium-ligand bond lengths [36,37,38]. Based on these results a functional could not be singled out for best performance.

Table 3: DFT calculated and experimental bond lengths (Å) and bond angles (°) around the rhodium centre of a single [Rh((C$_4$H$_3$S)COCHCO(C$_4$H$_3$S))(CO)(PPh$_3$)] molecule, obtained by a variety of functionals. Atom numbering is according to **Figure 1**.

Functional	Distance / Å				Angles / °			
	Rh1-O1	Rh1-O2	Rh1-C12	Rh1-P1	P1-Rh1-O1	O1-Rh1-O2	O2-Rh1-C12	C12-Rh1-P1
B3LYP	2.097	2.099	1.844	2.313	88.8	87.9	89.8	93.5
PW91	2.087	2.091	1.829	2.281	87.6	89.0	90.6	92.7
M06-D3	2.086	2.111	1.843	2.288	86.3	87.8	92.3	93.6
LC-BLYP	2.054	2.063	1.842	2.277	87.1	87.4	91.3	94.3
CAM-B3LYP	2.064	2.084	1.845	2.288	85.5	87.5	92.2	94.8
Crystal	*2.036*	*2.080*	*1.802*	*2.239*	*88.1*	*89.1*	*91.9*	*91.2*

3.3.2 Two [Rh((C$_4$H$_3$S)COCHCO(C$_4$H$_3$S))(CO)(PPh$_3$)] molecules

To further test the performance of the selected functionals (B3LYP, PW91, M06-D3, LC-BLYP and CAM-B3LYP), with respect to intermolecular geometrical parameters, two [Rh((C$_4$H$_3$S)COCHCO(C$_4$H$_3$S))(CO)(PPh$_3$)] molecules stacked together was optimized. The coordinates of two molecules that were involved in the more significant π-stacking, was selected

from the experimental crystal data and optimized with the selection of functionals. As an indication of the lateral shift between the two molecules (see **Figure 3**), the distance between the C6 carbon of the one molecule and the S1' sulphur of the other molecule was measured and summarized in **Table 4**. Functionals with dispersion (M06-D3) or long range corrections (LC-BLYP and CAM-B3LYP) performed much better in reproducing the experimental lateral shift between the two molecules. The LC-BLYP functional performed best with a slight deviation of 0.10 Å from the experimental crystal data. This functional was therefore used for the Natural Bond Orbitals (NBO) calculations and Bader's quantum theory of atoms in molecules (QTAIM) analysis.

Table 4: DFT calculated and experimental intermolecular distance (Å) of two [Rh((C$_4$H$_3$S)COCHCO(C$_4$H$_3$S))(CO)(PPh$_3$)] molecules, obtained by a variety of functionals.

Functional	Distance C6-S1'/ Å
B3LYP	6.171
PW91	4.153
M06-D3	3.719
LC-BLYP	3.771
CAM-B3LYP	3.662
Crystal	3.875

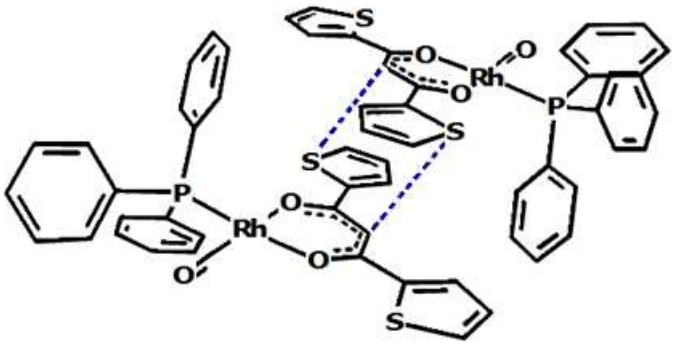

Figure 3: Visualisation of the lateral shift between two [Rh((C$_4$H$_3$S)COCHCO(C$_4$H$_3$S))(CO)(PPh$_3$)] molecules. The dotted lines indicated the intermolecular distance (Å) between the molecules, as summarized in **Table 4**.

3.3.3 NBO

Natural Bond Orbitals (NBO) calculations is presented here to describe the intermolecular interactions between two [Rh((C$_4$H$_3$S)COCHCO(C$_4$H$_3$S))(CO)(PPh$_3$)] molecules that result in the experimentally observed packing of the molecules in the solid state, as shown in **Figure 2**. A donor acceptor interaction LP(Rh) → BD*(C-H), between the lone pair (LP = 1-centre non-bonded lone

pair) on rhodium and the empty antibonding orbital (BD=2-centre bond) on C-H of the nearest thienyl group with second order perturbation theory interaction energy of 0.251 kJ/mol is obtained. This interaction involves the donation of electron density donation from the electron lone-pair on rhodium of d_{z^2} character, to an empty antibonding orbital on C-H. The interaction between the two [Rh((C$_4$H$_3$S)COCHCO(C$_4$H$_3$S))(CO)(PPh$_3$)] molecules is further strengthened by a donor acceptor interaction LP(Rh) → BD*(C-C) of 0.335 kJ/mol. BD*(C-C) is an empty antibonding orbital on two carbons of the nearest thienyl group to rhodium. Due to the symmetry, two LP(Rh) → BD*(C-H) and two LP(Rh) → BD*(C-C) interactions mutually strengthen the interaction between two [Rh((C$_4$H$_3$S)COCHCO(C$_4$H$_3$S))(CO)(PPh$_3$)] molecules near to each other, see **Figure 4**. An NBO analysis on the coordinates of the experimental two [Rh((C$_4$H$_3$S)COCHCO(C$_4$H$_3$S))(CO)(PPh$_3$)] molecules gave a slightly lower second order perturbation theory interaction energy of 0.209 kJ/mol for the latter donor acceptor LP(Rh) → BD*(C-C) interaction, while the energy of the LP(Rh) → BD*(C-H) donor acceptor is less than 0.1 kJ/mol. The weaker interactions obtained in the experimental system is due to the fact that in the experimental system the two molecules are ca 0.1 Å further apart than in the DFT optimized system, see **Table 5** for the intermolecular distances.

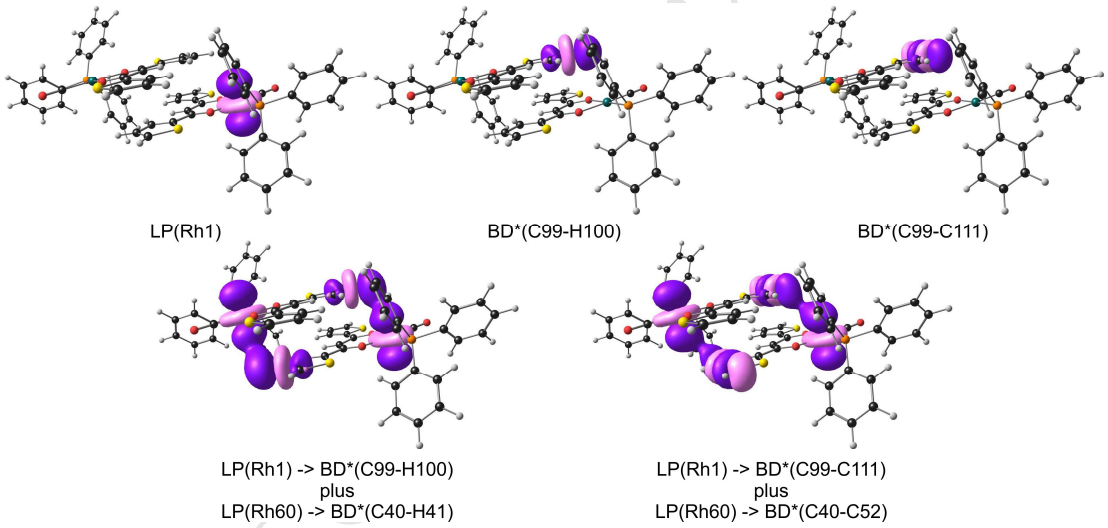

Figure 4: Top: The three types of NBOs involved in intermolecular interactions. Bottom: Visualisation of the two types of donor – acceptor NBO interactions between two molecular units of [Rh((C$_4$H$_3$S)COCHCO(C$_4$H$_3$S))(CO)(PPh$_3$)]. A contour of 0.03 e/Å^3 was used for the NBO plots. Colour code of atoms (online version): Rh (dark green), P (orange), S (yellow), C (black), O (red) and H (white). Atom numbering is according to Figure S1.

These donor – acceptor NBO interactions between two molecular units of [Rh((C$_4$H$_3$S)COCHCO(C$_4$H$_3$S))(CO)(PPh$_3$)] give an understanding how intermolecular NBO

overlap strengthen the interaction between two [Rh((C$_4$H$_3$S)COCHCO(C$_4$H$_3$S))(CO)(PPh$_3$)] molecules, leading to the experimental packing obtained for this complex.

Table 5: NBO second order interaction energies, E(2), and calculated NBO occupations, for the indicated donor-acceptor interactions between two molecular units of [Rh((C$_4$H$_3$S)COCHCO(C$_4$H$_3$S))(CO)(PPh$_3$)].

	E(2) / kJ·mol^{-1} DFT optimized structure	Experimental structure
LP(Rh $\boldsymbol{d_{z^2}}$) → BD*(CH) $_{\text{thienyl}}$	0.251	< 0.1
LP(Rh $\boldsymbol{d_{z^2}}$) → BD*(CC) $_{\text{thienyl}}$	0.335	0.209
Occupancy		
LP(Rh) / e$^-$	1.983	1.982
BD*(CH) $_{\text{thienyl}}$ / e$^-$	0.016	0.013
BD*(CC) $_{\text{thienyl}}$ / e$^-$	0.281	0.293
Intermolecular distance		
Rh – C$_{\text{CH-thienyl}}$	3.553	3.686
Rh – C$_{\text{CC-thienyl}}$	4.038	4.121

3.3.4 QTAIM

The intermolecular interactions between two [Rh((C$_4$H$_3$S)COCHCO(C$_4$H$_3$S))(CO)(PPh$_3$)] molecules were also analyzed with Bader's quantum theory of atoms in molecules (QTAIM), locating and characterizing the electronic density at bond critical points (BCPs) between the two units. The values of the charge density ρ(r) distribution and the corresponding Laplacian $\nabla^2\rho(r)$ at the bond critical point (BCP) allow the characterization of the chemical bonds between atoms in the molecules [39]. The formation of intermolecular hydrogen bonds is associated with a bond critical point between the hydrogen atom as donor atom and the acceptor atom (*e.g.* C or O), with the donor atom (H) linked by the concomitant bond path to the acceptor atom [40].

Ten (for DFT optimized model, eight for experimental model) intermolecular bond critical points, forming intermolecular bond paths, were obtained between two [Rh((C$_4$H$_3$S)COCHCO(C$_4$H$_3$S))(CO)(PPh$_3$)] molecules in the DFT optimized and experimental model respectively, see **Figure 5** for an illustration of the bond paths and **Table 6** for a summary of the topological parameters related to the intermolecular bond paths. Due to symmetry half of the intermolecular bond paths are similar to the other half of intermolecular bond paths:

(i) Two bond paths are intermolecular hydrogen bonds between a phenyl atom and a thienyl atom of the neighbouring molecule see **Figure 6** (and *vice versa*). In the DFT optimized model, both bond

paths between a phenyl carbon and a thienyl hydrogen of the neighbouring molecule. In the experimental model, one bond path is between a phenyl carbon and a thienyl hydrogen of the neighbouring molecule and the other between a phenyl hydrogen and a thienyl hydrogen of the neighbouring molecule. The electron density (ρ) at the bond critical points of the identified intermolecular hydrogen bonds of 0.003 – 0.005 e a_0^{-3} (**Table 6**) falls in the range of values reported for different types of hydrogen bonds, namely 0.002-0.035 e a_0^{-3} [40]. The value at the bond critical point of the DFT optimized model of the identified intermolecular hydrogen bonds of ca 0.018 for the Laplacian of the electron density ($\nabla^2\rho(r)$) falls in the range of values reported, 0.016-0.139 e a_0^{-5} [40], while that of the experimental model namely 0.011 e a_0^{-5} is slightly below the reported values.

(ii) Three (for DFT optimized model, two for experimental model) intermolecular bond paths are between an atom of the thienyl group of one molecule and an atom on the β-diketonato backbone of a neighbouring molecule, see **Figure 7**, with three (for DFT optimized model, two for experimental model) similar bond paths from the three atom on the β-diketonato backbone of the first molecule to atoms on the thienyl group of the second molecule. For the DFT optimized model the intermolecular bond paths are between a sulphur or a carbon on the thienyl group of one molecule and a carbon on the β-diketonato backbone of a neighbouring molecule, see **Figure 7** (a). For the experimental model two intermolecular bond paths exist between a carbon on the thienyl group of one molecule and a carbon on the β-diketonato backbone of a neighbouring molecule, see **Figure 7** (b), with two similar bond paths from two carbons on the β-diketonato backbone of the first molecule to two carbons on the thienyl group of the second molecule. The values of the ρ and $\nabla^2\rho(r)$ at the bond critical points of these intermolecular bond paths are similar to the values obtained for the intermolecular hydrogen bonds and the reported ranges for different types of hydrogen bonds [40].

These identified QTAIM intermolecular bond paths explain how the interaction between two molecular units of $[Rh((C_4H_3S)COCHCO(C_4H_3S))(CO)(PPh_3)]$ is strengthen, leading to the experimental packing obtained for this complex.

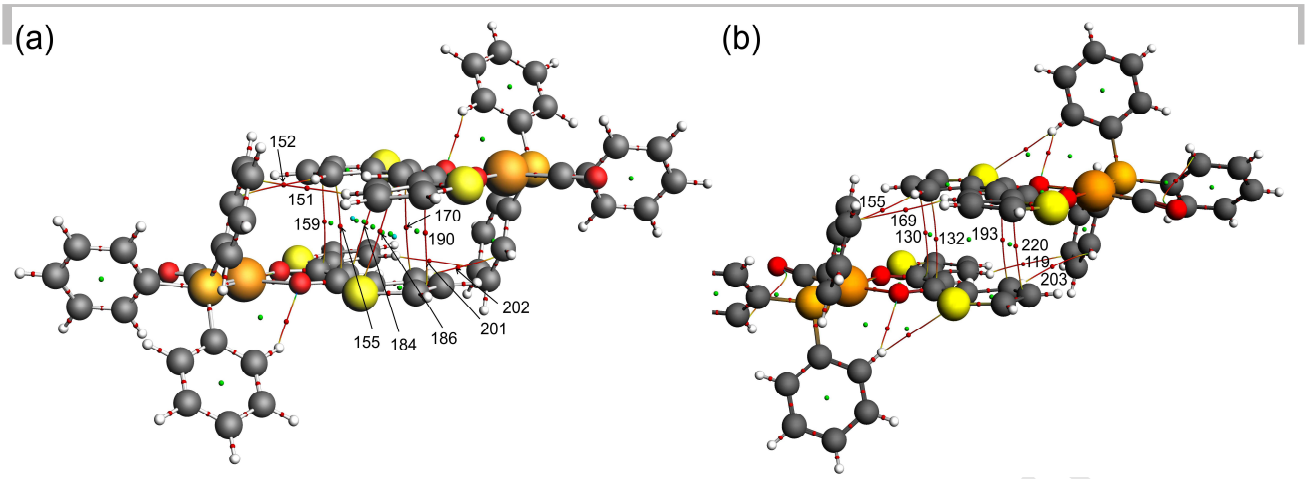

Figure 5: QTAIM determined inter-molecular bond-paths (BP) and bond critical points (CP in red) between two [Rh((C$_4$H$_3$S)COCHCO(C$_4$H$_3$S))(CO)(PPh$_3$)] units in (a) the DFT optimized model and (b) the experimental system. Ring critical points are shown in green. The colour of the bond-paths changes according to electron density from blue (high density) to green to red (low density).

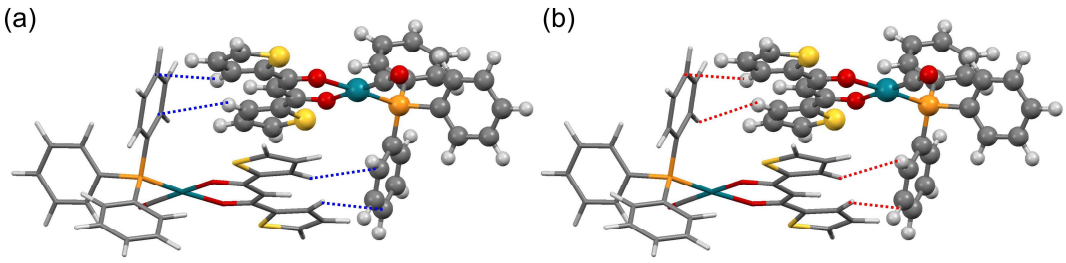

Figure 6: Illustration of the four inter-molecular QTAIM bond-paths (BP) between two [Rh((C$_4$H$_3$S)COCHCO(C$_4$H$_3$S))(CO)(PPh$_3$)] units involving a phenyl carbon on one molecule and a thienyl hydrogen on the other molecule in (a) the DFT optimized model and (b) the experimental system.

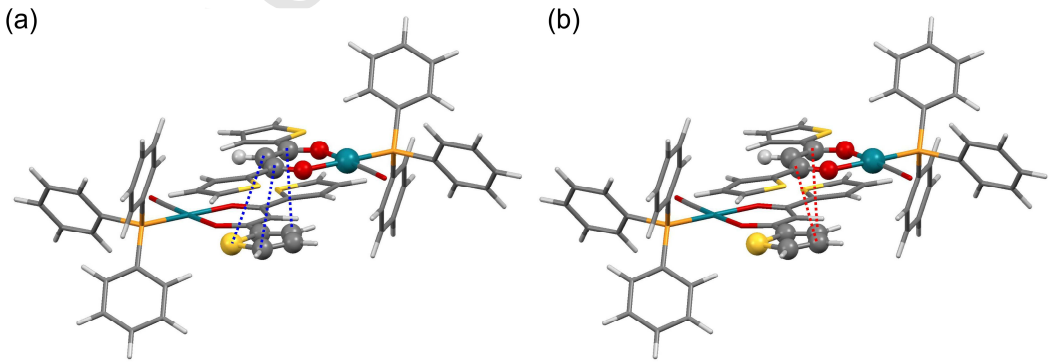

Figure 7: Illustration of selected inter-molecular QTAIM bond-paths (BP) between a thienyl group and the β-diketonato backbone of two [Rh((C$_4$H$_3$S)COCHCO(C$_4$H$_3$S))(CO)(PPh$_3$)] units in (a) the DFT optimized model and (b) the experimental system.

Table 6: Topological parameters of the QTAIM calculated intermolecular bonds between two [Rh((C$_4$H$_3$S)COCHCO(C$_4$H$_3$S))(CO)(PPh$_3$)] units. The numbers of the critical points (CP) are shown in Figure 5.

	Atoms involved	**inter-atomic distance**	**BP length / Å**	**ρ / e a_0^{-3}**	**$\nabla^2\rho$ / e a_0^{-5}**
DFT optimized structure					
Hydrogen bonds between a phenyl carbon and a thienyl hydrogen.					
CP # 151	C115(Ph)-H11(Th)	2.820	2.846	0.0054	0.0170
CP # 152	C105(Ph)-H9(Th)	2.843	3.004	0.0055	0.0183
CP # 201	H70(Th)-C56(Ph)	2.820	2.845	0.0054	0.0170
CP # 202	H68(Th)-C46(Ph)	2.843	3.007	0.0055	0.0183
BP between a thienyl group and the β-diketonato backbone					
CP # 155	C8(Th)-C81(beta)	3.359	3.797	0.0056	0.0179
CP # 159	C52(Th)-C82(beta)	3.407	3.936	0.0057	0.0188
CP # 170	C67(Th)-C22(beta)	3.360	3.802	0.0055	0.0178
CP # 184	C86(metine beta)-S4	3.772	3.785	0.0043	0.0138
CP # 186	S63-C27(methine beta)	3.771	3.784	0.0043	0.0138
CP # 190	C111(Th)-C23(beta)	3.406	3.925	0.0057	0.0188
Experimental structure					
Hydrogen bonds between a phenyl carbon and a thienyl hydrogen.					
CP # 169	C115(Ph)-H11(Th)	3.107	3.145	0.0032	0.0108
CP # 155	H106(Ph)-H9(Th)	2.725	2.990	0.0026	0.0101
CP # 119	H70(Th)-C56(Ph)	3.107	3.145	0.0032	0.0108
CP # 203	H68(Th)-H47(Ph)	2.725	2.990	0.0026	0.0101
BP between a thienyl group and the β-diketonato backbone					
CP # 132	C8(Th)-C81(beta)	3.373	3.672	0.0055	0.0169
CP # 130	C40(Th)-C82(beta)	3.425	3.936	0.0054	0.0173
CP # 193	C67(Th)-C22(beta)	3.373	3.672	0.0055	0.0169
CP # 220	C99(Th)-C23(beta)	3.425	3.936	0.0054	0.0173

4 Conclusion

The orientation of the two aromatic thienyl groups on the β-diketonato backbone of [Rh((C$_4$H$_3$S)COCHCO(C$_4$H$_3$S))(CO)(PPh$_3$)] deviates very slightly from the plane through the β-diketonato backbone. The near planar orientation of the two aromatic thienyl groups and the β-diketonato backbone leads to stacking of [Rh((C$_4$H$_3$S)COCHCO(C$_4$H$_3$S))(CO)(PPh$_3$)] in one

dimensional linear chains in the solid state, with slightly slipped π-stacking of the thienyl groups and the β-diketonato backbone. Each β-diketonato moiety is involved in two different π-π interactions, the most dominating one with the thienyl ring that includes S1 (inter-centroid distance 3.753(2) Å), the secondary weaker π-π interaction with the thienyl ring that includes S2 (inter-centroid distance 4.797(2) Å). Theoretical QTAIM calculations showed that weak intermolecular bond paths exist between a sulphur or a carbon on the thienyl group of one molecule and a carbon on the β-diketonato backbone of a neighbouring molecule, and that the observed packing of the molecules are further strengthened by intermolecular hydrogen bonds between a phenyl carbon and a thienyl hydrogen of the neighbouring molecule. The orientation of the thienyl groups make donor – acceptor NBO interactions the lone pair on rhodium and the empty antibonding orbital on C-H of the nearest thienyl group possible. The interaction between the two [Rh((C_4H_3S)COCHCO(C_4H_3S))(CO)(PPh_3)] molecules is further strengthened by a second donor – acceptor NBO interaction between the rhodium lone pair and an empty antibonding orbital on two carbons of the nearest thienyl group to rhodium.

Supporting Information

Crystallographic data has been deposited at the Cambridge Crystallographic Data Centre with number 1811145. Copies can be obtained, free of charge, on application to CCDC, 12 Union Road, Cambridge CB2 1EZ, UK [fax: +44 (0)1223 336033 or ww.ccdc.cam.ac.uk/products/csd/request/]. Selected crystallographic data and optimized coordinates of the DFT calculations are given in the Supporting Information.

Acknowledgements

This work has received support from the South African National Research Foundation and the Central Research Fund of the University of the Free State, Bloemfontein, South Africa. The Norwegian supercomputing program NOTUR (Grant No. NN4654K), are gratefully acknowledged for computer time.

References

[1] J. Swanston, Thiophene, Ullmann's Encyclopedia of Industrial Chemistry, Wiley-VCH Verlag GmbH & Co. KGaA, Weinheim, Germany, 2006, Vol. 36, pp. 657-669. DOI: 10.1002/14356007.a26_793.pub2
[2] M. Al-Anber, B. Milde, W. Alhalasah, H. Lang, R. Holze, Electrochemical and DFT-studies of substituted thiophenes, Electrochimica Aca 53 (2008) 6038-6047. DOI: 10.1016/j.electacta.2008.02.042
[3] M.M. Conradie, A.J. Muller, J. Conradie, Thienyl-containing β-diketones: synthesis, characterization, crystal structure, keto-enol kinetics, S. Afr. J. Chem. 61 (2008) 13-21. http://www.journals.co.za/sajchem/
[4] M.M. Conradie, J. Conradie, Methyl Iodide Oxidative Addition to Monocarbonylphosphine [Rh((C_4H_3S)COCHCOR)(CO)(PPh_3)] Complexes, utilizing UV/vis and IR Spectrophotometry and NMR Spectroscopy to identify Reaction Intermediates. R = C6H5 or C4H3S, Inorg. Chim. Acta. 361 (2008) 2285-2295. DOI:10.1016/j.ica.2007.10.052
[5] H. Ferreira, M.M. Conradie, J. Conradie, Electrochemical study of Carbonyl Phosphine β-Diketonato Rhodium(I) Complexes, Electrochim. Acta 113 (2013) 519-526. DOI:10.1016/j.electacta.2013.09.099
[6] APEX2 (including SAINT and SADABS), Bruker AXS Inc., Madison, WI, 2012.
[7] G.M. Sheldrick, A short history of SHELX, Acta Cryst. Sect. A 64 (2008) 112-122. DOI:10.1107/S0108767307043930
[8] M.J. Frisch, G.W. Trucks, H.B. Schlegel, G.E. Scuseria, M.A. Robb, J.R. Cheeseman, G. Scalmani, V. Barone, B. Mennucci, G.A. Petersson, H. Nakatsuji, M. Caricato, X. Li, H.P. Hratchian, A.F. Izmaylov, J. Bloino, G. Zheng, J.L. Sonnenberg, M. Hada, M. Ehara, K. Toyota, R. Fukuda, J. Hasegawa, M. Ishida, T. Nakajima, Y. Honda, O. Kitao, H. Nakai, T. Vreven, J.A. Montgomery (Jr), J.E. Peralta, F. Ogliaro, M. Bearpark, J.J. Heyd, E. Brothers, K.N. Kudin, V.N. Staroverov, T. Keith, R. Kobayashi, J. Normand, K. Raghavachari, A. Rendell, J.C. Burant, S.S. Iyengar, J. Tomasi, M. Cossi, N. Rega, J.M. Millam, M. Klene, J.E. Knox, J.B. Cross, V. Bakken, C. Adamo, J. Jaramillo, R. Gomperts, R.E. Stratmann, O. Yazyev, A.J. Austin, R. Cammi, C. Pomelli, J.W. Ochterski, R.L. Martin, K. Morokuma, V.G. Zakrzewski, G.A. Voth, P. Salvador, J.J. Dannenberg, S. Dapprich, A.D. Daniels, O. Farkas, J.B. Foresman, J.V. Ortiz, J. Cioslowski, D.J. Fox, Gaussian 09, Revision D.01, Gaussian Inc., Wallingford CT, 2010.
[9] J.P. Perdew, J.A. Chevary, S.H. Vosko, K.A. Jackson, M.R. Pederson, D.J. Singh, C. Fiolhais, Atoms, molecules, solids, and surfaces: Applications of the generalized gradient approximation for exchange and correlation, Physical Review B 46 (1992) 6671-6687. Erratum: J.P. Perdew, J.A. Chevary, S.H. Vosko, K.A. Jackson, M.R. Perderson, D.J. Singh, C. Fiolhais, Physical Review B 48 (1993) 4978. DOI:10.1103/PhysRevB.46.6671
[10] B. Miehlich, A. Savin, H. Stoll, H. Preuss, Results obtained with the correlation-energy density functionals of Becke and Lee, Yang and Parr, Chem. Phys. Lett. 157 (1989) 200-06. DOI:10.1016/0009-2614(89)87234-3.
[11] H. Iikura, T. Tsuneda, T. Yanai, K. Hirao, Long-range correction scheme for generalized-gradient-approximation exchange functionals, J. Chem. Phys. 115 (2001) 3540-44. DOI:10.1063/1.1383587
[12] A.D. Becke, Density-functional exchange-energy approximation with correct asymptotic behavior, Phys. Rev. A 38 (1988) 3098–3100. DOI:10.1103/PhysRevA.38.3098
[13] C.T. Lee, W.T. Yang, R.G. Parr, Development of the Colle-Salvetti correlation-energy formula into a functional of the electron density, Phys. Rev. B 37 (1988) 785–789. DOI:10.1103/PhysRevB.37.785
[14] Y. Zhao, D.G. Truhlar, The M06 suite of density functionals for main group thermochemistry, thermochemical kinetics, noncovalent interactions, excited states, and transition elements: two new functionals and systematic testing of four M06-class functionals and 12 other functionals, Theor. Chem. Acc. 120 (2008) 215-41. DOI:10.1007/s00214-007-0310-x

[15] S. Grimme, J. Antony, S. Ehrlich, H. Krieg, A consistent and accurate ab initio parametrization of density functional dispersion correction (DFT-D) for the 94 elements H-Pu. J. Chem. Phys. 132 (2010) 154104-154104. DOI:10.1063/1.3382344
[16] A.D. Becke, Density-functional thermochemistry. III. The role of exact exchange, J. Chem. Phys. 98 (1993) 5648-5652. DOI:10.1063/1.464913
[17] C. Lee, W. Yang, R.G. Parr, Development of the Colle-Salvetti correlation-energy formula into a functional of the electron density, Phys. Rev. B 37 (1988) 785-789. DOI:10.1103/PhysRevB.37.785
[18] T. Yanai, D. Tew, N. Handy, A new hybrid exchange-correlation functional using the Coulomb-attenuating method (CAM-B3LYP), Chem. Phys. Lett. 393 (2004) 51-57. DOI:10.1016/j.cplett.2004.06.011.
[19] (a) T.H. Dunning Jr., P.J. Hay, Methods of Electronic Structure, in: H.F. Schaefer III (Ed.), Modern Theoretical Chemistry, Plenum, New York, NY, USA, 1977, vol. 3, pp. 1-28.
(b) P.J. Hay, W.R. Wadt, *Ab initio* effective core potentials for molecular calculations. Potentials for the transition metal atoms Sc to Hg, J. Chem. Phys. 82 (1985) 270-283. DOI:10.1063/1.448799
(c) W.R. Wadt, P.J. Hay, *Ab initio* effective core potentials for molecular calculations. Potentials for main group elements Na to Bi, J. Chem. Phys. 82 (1985) 284-298. DOI:10.1063/1.448800
(d) P.J. Hay, W.R. Wadt, *Ab initio* effective core potentials for molecular calculations. Potentials for K to Au including the outermost core orbitals, J. Chem. Phys. 82 (1985) 299-310. DOI:10.1063/1.448975
[20] O.V. Sizova, Y.S. Varshavskii, A.B. Nikol'skii, Binuclear Rhodium(I) Carbonyl Carboxylate Complexes: DFT Study of Structural and Spectral Properties, Russian Journal of Coordination Chemistry 31 (2005) 875–883. DOI:10.1007/s11173-005-0185-0
[21] K.H. Hopmann, J. Conradie, A Density Functional Theory Study of Substitution at the Square-Planar Acetylacetonato-dicarbonyl-rhodium(I) complex, Organometallics 28 (2009) 3710–3715. DOI:10.1021/om900133s
[22] K.H. Hopmann, N.F. Stuurman, A. Muller, J. Conradie, Substitution and Isomerisation of Asymmetric β-Diketonato Rhodium (I) Complexes: A Crystallographic and Computational Study, Organometallics 29 (2010) 2446–2458. DOI:10.1021/om1000138
[23] E.D. Glendening, J.K. Badenhoop, A.E. Reed, J.E. Carpenter, J.A. Bohmann, C.M. Morales, F. Weinhold, NBO 3.1, Theoretical Chemistry Institute, University of Wisconsin, Madison, WI, USA, 2001.
[24] R.F.W. Bader, A quantum theory of molecular structure and its applications, Chemical Reviews 91 (1991) 893-928. DOI:10.1021/cr00005a013
[25] F. Cortés-Guzmán, R.F.W. Bader, Complementarity of QTAIM and MO theory in the study of bonding in donor–acceptor complexes, Coordination Chemistry Reviews 249 (2005) 633-662. DOI:10.1016/j.ccr.2004.08.022
[26] J.I. Rodríguez, R.F.W. Bader, P.W. Ayers, C. Michel, A.W. Götz, C. Bo, A high performance grid-based algorithm for computing QTAIM properties, Chemical Physics Letters 472 (2009) 149-152. DOI:10.1016/j.cplett.2009.02.081
[27] G. te Velde, F.M. Bickelhaupt, S.J.A. van Gisbergen, C.F. Guerra, E.J. Baerends, J.G. Snijders, T. Ziegler, Chemistry with ADF, Journal of Computational Chemistry 22 (2001) 931-967. DOI:10.1002/jcc.1056
[28] C.F. Guerra, J.G. Snijders, G. te Velde, E.J. Baerends, Towards an order-N DFT method, Theor. Chem. Acc. 99 (1998) 391-403. DOI:10.1007/s002140050353
[29] ADF2016, SCM, Theoretical Chemistry, Vrije Universiteit, Amsterdam, The Netherlands, 2016. http://www.scm.com
[30] Mercury CSD 3.10.1 (Build 168220), http://www.ccdc.cam.ac.uk/mercury/
[31] C.F. Macrae, I.J. Bruno, J.A. Chisholm, P.R. Edgington, P. McCabe, E. Pidcock, L. Rodriguez-Monge, R. Taylor, J. van de Streek and P. A. Wood, J. Appl. Cryst. 41 (2008) 466-470.

[32] Chemcraft Version 1.8 (Built 428), https://www.chemcraftprog.com/
[33] (a) Ph. Serp, M. Hernandez, B. Richard. Ph. Kalck, A Facile Route to Carbonylhalogenometal Complexes (M = Rh, Ir, Ru, Pt) by Dimethylformamide Decarbonylation, Eur. J. Inorg. Chem. 9 (2001) 2327-2336. DOI:10.1002/1099-0682(200109)2001:9<2327::AID-EJIC2327>3.0.CO;2-D
(b) Y.S. Varshavsky, T.G. Cherkasova, Remarks on the process of homogeneous carbonylation of rhodium compounds by *N*,*N*-dimethylformamide, J. Organomet. Chem. 692 (2007) 887-893. DOI:10.1016/j.jorganchem.2006.10.040
[34] Cambridge Structural Database (CSD), Version 5.38, May 2017 update, Cambridge, UK, 2017.
[35] W.J. Hehre, A Guide to Molecular Mechanisms and Quantum Chemical Calculations, Wavefunction Inc., Irvine, CA, USA, 2003, pp. 153, 181.
[36] M.M. Conradie, J. Conradie, Methyl Iodide Oxidative Addition to Rhodium(I) Complexes: a DFT and NMR Study of [Rh(FcCOCHCOCF$_3$)(CO)(PPh$_3$)] and the Rhodium(III) Reaction Products, S. Afr. J. Chem. 61 (2008) 102-111. http://www.journals.co.za/sajchem/
[37] M.M. Conradie, J. Conradie, Stereochemistry of the Reaction Products of the Oxidative Addition Reaction of Methyl Iodide to [Rh((C$_4$H$_3$S)COCHCOR)(CO)(PPh$_3$)]: a NMR and Computational Study. R = CF$_3$, C$_6$H$_5$, C$_4$H$_3$S, Inorg. Chim. Acta 362 (2009) 519-530. DOI:10.1016/j.ica.2008.04.046
[38] M.M. Conradie, J. Conradie, A Density Functional Theory Study of the Oxidative Addition of Methyl Iodide to Square Planar [Rh(acac)(P(OPh)$_3$)$_2$] complex and simplified model systems, J. Organomet. Chem. 695 (2010) 2126-2133. DOI:10.1016/j.jorganchem.2010.05.021
[39] R.F.W. Bader, A Bond Path: A Universal Indicator of Bonded Interactions, J. Phys. Chem. A 102 (1998) 7314–7323. DOI:10.1021/jp981794v
[40] (a) M.T. Caroll, R.F.W. Bader, An analysis of the hydrogen bond in BASE-HF complexes using the theory of atoms in molecules, Mol. Phys. 65 (1988) 695-722. DOI:10.1080/00268978800101351
(b) M.T. Caroll, C. Chang, R.F.W. Bader, Prediction of the structures of hydrogen-bonded complexes using the laplacian of the charge density, Mol. Phys. 63 (1988) 387-405. DOI:10.1080/00268978800100281
(c) R.F.W. Bader, H. Essén, The characterization of atomic interactions, J. Chem. Phys. 80 (1984) 1943-1960. DOI:10.1063/1.446956
(d) P.L.A. Popelier, R.F.W. Bader, The existence of an intramolecular C-H-O hydrogen bond in creatine and carbamoyl sarcosine, Chem. Phys. Lett. 189 (1992) 542-548. DOI:10.1016/0009-2614(92)85247-8
(e) U. Koch, P.L.A. Popelier, Characterization of C-H-O Hydrogen Bonds on the Basis of the Charge Density, J. Phys. Chem. 99 (1995) 9747–9754. DOI:10.1021/j100024a016

Highlights

Packing in pairs with weak intermolecular interaction

AIM bonding paths indicating intermolecular bonding paths

NBO shows intermolecular donor-acceptor interaction